

EVALUATION OF STATISTICAL MODELS FOR CLEAR-AIR SCINTILLATION PREDICTION USING OLYMPUS SATELLITE MEASUREMENTS

GEOFFROY PEETERS

Institute of Research and Coordination in Acoustic and Music (IRCAM), Department of Analysis and Synthesis, Place Igor Strawinsky 1, 75004 Paris, France

FRANK SILVIO MARZANO AND GIOVANNI d'AURIA

Dipartimento di Ingegneria Elettronica, Università 'La Sapienza' di Roma, Via Eudossiana 18, 00184 Rome, Italy

CARLO RIVA

Dipartimento di Elettronica e Informazione, Politecnico di Milano, Piazza Leonardo da Vinci 32, 20133 Milan, Italy

D. VANHOENACKER-JANVIER

Microwaves Laboratory, Université Catholique de Louvain, Batiment Maxwell 3, B-1348 Louvain-la-Neuve, Belgium

SUMMARY

The objective of this study is to evaluate and to compare some of the statistical models for the monthly prediction of clear-air scintillation variance and amplitude from ground meteorological measurements. Two new statistical methods, namely the direct and the modelled physical-statistical prediction models, are also introduced and discussed. They are both based on simulated data of received scintillation power derived from a large historical radiosounding set, acquired in a mid-latitude site. The long-term predictions derived from each model are compared with measurements from the Olympus satellite beacons at the Louvain-la-Neuve site at 12.5 and 29.7 GHz and at the Milan site at 19.77 GHz during 1992. The model intercomparison is carried out by checking the assumed best-fitting probability density function for the variance and log-amplitude fluctuations and analysing the proposed relationships between scintillation parameters and ground meteorological measurements. Results are discussed in order to understand the potentials and the limits of each prediction model within this case study. The agreement with Olympus measurements is found to be mainly dependent on the proper parametrization of prediction models to the radiometeorological variables along the earth-satellite path. ©1997 by John Wiley & Sons, Ltd.

KEY WORDS: scintillation; prediction models; Olympus satellite

1. INTRODUCTION

The rapid development of telecommunications and the increasing demands for larger channel capacity is forcing the use of beacon frequencies in the K band.^{1,2} At frequencies above 10 GHz, a satellite-earth link crossing the atmosphere is affected in several ways: attenuation caused by a combination of absorption caused by gases (water vapour and oxygen) and extinction caused by hydrometeors, and depolarization caused by atmospheric anisotropies and scintillation.^{3–6} Scintillation phenomena result from atmospheric turbulence, causing random variations of the amplitude, phase and angle of arrival of the received signal in a random way.⁷ As expected and proved by various experiments, clear-air scintillation increases as the elevation angle decreases and the beacon frequency increases.^{8–10} The possible presence of cloud liquid water along the path, and even the development of convective rain processes, may be a source of scintillation enhancement.^{3,11} Intermittence effects can also play a significant role in determining the scintillation intensity.^{12,13}

In the past few years many microwave propagation experiments have been carried out to evaluate the impact of tropospheric scintillations (and, in general, of atmospheric phenomena) on the budget design of satellite links.^{14,15} These experiments usually involve large resources and are generally not easy to set up for each link. To cope with these problems, there has been a growing interest in developing statistical methods for predicting tropospheric scintillations directly from meteorological data. On one hand, these prediction models can be based on experimental data of a collection of beacon sites whose results are generally extended to other sites and frequencies by means of empirical functions.^{16–20} On the other hand, numerical models of the interaction between microwave radiation and turbulent atmosphere can provide a tool to evaluate the received scintillation power and its spectrum in a given frequency band and for a given elevation angle.^{21–23} Generally, these interaction models are a function of atmospheric parameters available at ground or from a radiosonde. The radiosoundings can represent a valuable data source because they

can give a complete characterization of the vertical atmospheric structure, even though large historical data sets are not always available for all the receiving stations. Indeed, the atmospheric state could be also derived by remote sensing techniques, as ground-based radars²⁴ and microwave radiometers.⁴ Ground meteorological data are much easier to acquire and to collocate at the beacon site which is the reason why prediction models based on them are widely used and tested.

In this paper, we study the tropospheric amplitude scintillation occurring for frequencies higher than 10 GHz and for elevation angles above 10° in clear-air conditions. Most of the commonly-used prediction models of clear-air scintillation which have been proposed during the past few years are reviewed and applied to Olympus measurements during 1992 at various sites. Starting from the current state-of-the-art, we also present two new prediction models, the direct and the modelled physical-statistical prediction models, based on numerical simulations of the received scintillation power along a slant path through an intermittent turbulent stratified atmosphere described by a large vertical profile of atmospheric variables, obtained by radiosonde balloons (radiosounding database). By means of regression techniques, the new prediction models statistically relate the simulated scintillation intensity to ground meteorological data. After having described the set of Olympus data used in this work, we use them in order to check the validity of their assumptions and compare the results of the prediction models considered within this case study.

2. STATISTICAL PREDICTION MODELS

A well established hypothesis is to assume that the log-amplitude fluctuation χ (in dB) follows a Gaussian probability density function (PDF), which is stationary in the short term (order of a few minutes).^{10,16} However, over a longer period of time the standard deviation σ_χ (hereinafter also called scintillation intensity) of χ varies according to its own PDF $p(\sigma_\chi)$, so that the cumulative distribution $P(\chi > \chi_0)$ of χ can be written as:¹⁰

$$P(\chi > \chi_0) = \int_{\chi_0}^{\infty} \int_0^{\infty} p(\chi|\sigma_\chi) \cdot p(\sigma_\chi) d\sigma_\chi d\chi \quad (1)$$

where χ_0 is a given threshold value and $p(\chi|\sigma_\chi)$ is the condition PDF of χ given σ_χ . Equation (1) can also be written in terms of the scintillation variance σ_χ^2 of χ , instead of the intensity σ_χ . In order to compute this cumulative distribution, it is necessary to know which is the PDF followed by σ_χ and which are the parameters of this PDF (e.g. the mean and the standard deviation). Most of the statistical models usually try to link the parameters of this PDF to ground meteorological measurements, such as temperature, relative humidity and wind velocity.

By using statistical parameters averaged over a long period of time (typically a week or a month), a stronger correlation with the ground meteorological measurements can be achieved. This is the main reason why long-term statistical prediction methods are generally proposed, even though diurnal variation analysis of scintillation is gaining increasing attention in research activities.⁶

2.1. Karasawa and ITU-R models

The following prediction models are described together because they are very similar to each other. They both give a statistical method for the prediction of the cumulative distribution of χ based on the assumption of a Gaussian PDF for χ in the short term and a Gamma PDF for σ_χ in the longterm.

The model proposed in Reference 16, hereinafter for simplicity called the 'Karasawa model', is assumed to be valid for frequencies ranging from 7 to 14 GHz and elevation angles ranging from 4° to 30°. The regression between the monthly averaged value $\overline{\sigma_\chi}$ of σ_χ (in dB) and the wet-term refractive index N_{wet} (in percentage) at the surface is:

$$\overline{\sigma_\chi} = \sqrt{G(R_{eff})} \cdot f^{0.45} \cdot \sin^{-1.3} \theta \cdot (0.0032 + 0.11856 \times N_{wet}) \quad (2)$$

where $R_{eff} = 0.75 (D_a/2)$ is the effective radius of circular antenna aperture of diameter D_a (in m), f is the beacon frequency (in GHz) and θ is the elevation angle. The antenna aperture averaging factor $G(R_{eff})$ is given by:

$$\begin{aligned} G(R_{eff}) &= 1.0 - 1.4 \cdot \left(\frac{R_{eff}}{\sqrt{\lambda L}} \right) \quad \text{for } 0 \leq \frac{R_{eff}}{\sqrt{\lambda L}} \leq 0.5 \\ &= 0.5 - 0.4 \cdot \left(\frac{R_{eff}}{\sqrt{\lambda L}} \right) \quad \text{for } 0.5 \leq \frac{R_{eff}}{\sqrt{\lambda L}} \leq 1.0 \\ &= 0.1 \quad \text{for } 1.0 \leq \frac{R_{eff}}{\sqrt{\lambda L}}, \end{aligned} \quad (3)$$

where λ is the beacon wavelength (in m), L is the slant distance over curve earth to height H (in m) of a horizontal turbulent layer ($H = 2000$ m is suggested) and $R_{eff} = 0.75 D_a/2$, being D_a the antenna diameter (in m).

The International Telecommunication Union model,¹⁷ described in Report 718-3 and hereinafter cited as 'ITU-R model' for brevity, is mostly derived from the previous Karasawa model, but is applicable to frequencies ranging from 7 to 20 GHz and is characterized by the following regression between the monthly averaged value of σ_χ and surface N_{wet} :

$$\overline{\sigma_\chi} = \sqrt{G(R_{eff})} \cdot f^{0.583} \cdot \sin^{-1.2} \theta \cdot (0.0036 + 0.103 N_{wet}) \quad (4)$$

The ITU-R antenna aperture averaging factor is also different and is given by:

$$G(x) = 3.86 (x^2 + 1)^{11/12} \cdot \sin\left(\frac{11}{6} \arctan\left(\frac{1}{x}\right)\right) - 7.08x^{5/6} \quad (5)$$

where $x = 1.464 \cdot \left(\frac{R_{\text{eff}}}{\sqrt{\lambda L}}\right)^2$. Notice that the value of

H is taken to be equal to 1000 m and $R_{\text{eff}} = R_a \sqrt{\eta}$ with R_a the antenna radius (in m) and η the antenna radiation efficiency. Even though equations (3) and (5) are derived from different approaches, they give very similar results.³

For the rest, the Karasawa and ITU-R models are almost identical. In fact, both assume the following relationship between the variance of σ_χ and the square of its mean value $\overline{\sigma_\chi}$:

$$\sigma_{\sigma_\chi}^2 = 0.1 \overline{\sigma_\chi}^2 \quad (6)$$

and then compute the parameters of the Gamma function (see References 16 and 17 for further details).

By using some mathematical properties of the Gamma PDF in order to invert equation (1) numerically, the value of the signal level χ exceeded for a percentage P of time can be expressed by:

$$\chi(P, \overline{\sigma_\chi}) = \eta(P) \times \overline{\sigma_\chi}(f, \theta, D_a, \text{Nwet}) \quad (7)$$

where $\eta(P)$ is the time percentage factor. This factor may be divided into two parts, the signal fluctuation ‘enhancement’ and the signal fluctuation ‘fading’, having the following expressions.

For $50 \leq P \leq 99.99$ and only for the Karasawa model, the signal fluctuation ‘enhancement’ is:¹⁶

$$\begin{aligned} \eta(P) = & -0.0597 \cdot (\log(100 - P))^3 - 0.0835 \\ & \cdot (\log(100 - P))^2 \\ & - 1.258 \cdot (\log(100 - P)) + 2.672 \end{aligned} \quad (7a)$$

For $0.01 \leq P \leq 50$ and for both the models, the signal fluctuation ‘fading’ is:

$$\begin{aligned} \eta(P) = & -0.061 \cdot (\log P)^3 - 0.072 \cdot \\ & (\log P)^2 - 1.71 \cdot (\log P) + 3.0 \end{aligned} \quad (7b)$$

Note that the regression coefficients of equation (7) have been experimentally derived.

2.2. Ortgies models

The methods proposed by Ortgies for the prediction of the cumulative distribution of σ_χ^2 are derived from Olympus measurements at Darmstadt using the beacons at 12.5 GHz, 20 GHz and 30 GHz and

antennae with diameters of 0.6 m, 1.8 m and 3.7 m, respectively.^{18,19} The prediction models are applicable for elevation angles from 6.5° to 30°, as deduced by experimental results.

The methods predict the scintillation variance σ_χ^2 (instead of the scintillation intensity, as before), and, according to it, the variation of σ_χ^2 over a long period of time (of the order of a month) follows a log-normal PDF, i.e.:

$$p(\sigma_\chi^2) = \frac{1}{\sqrt{2\pi s \sigma_\chi^2}} \exp\left(-\frac{(\ln(\sigma_\chi^2) - \mu)^2}{2s^2}\right) \quad (8)$$

where μ and s are the mean and standard deviation of $\ln(\sigma_\chi^2)$, respectively. As known, if σ_χ^2 follows a log-normal PDF, then $\ln(\sigma_\chi^2)$ follows a normal PDF and the mean and standard deviation of $\ln(\sigma_\chi^2)$ are directly the μ and s parameters of the log-normal PDF. This explains why the model regressions are made directly on $\ln(\sigma_\chi^2)$. From another point of view, thinking of the scintillation process as a multiplicative random process, the arithmetic average of $\ln(\sigma_\chi^2)$ is equivalent to the geometric average of σ_χ^2 .

Two direct relations between monthly mean value μ of $\ln(\sigma_\chi^2)$ are proposed. The first links μ to surface Nwet and is given by (hereinafter, called ‘Ortgies-N model’):¹⁸

$$\begin{aligned} \mu = & \ln(G(R_{\text{eff}}) \cdot \sin(\theta)^{-2.4} \cdot f^{1.21}) \\ & - 13.45 + 0.0462 \cdot \text{Nwet} \end{aligned} \quad (9)$$

whereas the second relates it to surface temperature T (in °C) and is given by (hereinafter, called ‘Ortgies-T model’):¹⁹

$$\mu = \ln(G(R_{\text{eff}}) \cdot \sin(\theta)^{-2.4} \cdot f^{1.21}) - 12.5 + 0.0865 \cdot T \quad (10)$$

In both equation (9) and equation (10) the frequency scaling factor is very close to that of the ITU-R (see equation (4)) and the antenna aperture averaging factor is given by ITU-R.¹⁷ Notice that both Ortgies models have been set up by using data from the Olympus beacons in Darmstadt, Germany.

Concerning the parameter s in equation (8)), it can in general be expressed with respect to the average intensity of scintillation as follows:²⁵

$$s^2 = \left[\frac{(\sigma_{\sigma_\chi^2})^2 + (\overline{\sigma_\chi^2})^2}{(\overline{\sigma_\chi^2})^2} \right] \quad (11)$$

Ortgies experimentally concludes that s appears to be independent of system parameters and meteorological quantities so that s is taken as a constant value equal to 1.01. Note that using the Karasawa assumption given by equation (6), it would have given roughly $s \cong 0.3$ (we cannot exactly calculate it because equation (11) requires

mean variances). The estimate of scintillation log-amplitude probability, given in equation (1), is derived by assuming a Gaussian distribution for χ and a log-normal distribution for σ_χ^2 (see next equation (18)).

2.3. DPSP and MPSP models

Two new statistical models for the prediction of the monthly mean value of the scintillation variance from ground measurements are illustrated here. They are both based on numerical simulations of scintillation power as received by a beacon station where a large radiosounding data base is available. The physical model behind these simulations was developed by Tatarskii,⁷ refined for the intermittent turbulence hypothesis in References 13 and 22. If the Taylor 'frozen-in' hypothesis is assumed and the atmospheric turbulence lies in the inertial sub-range and is intermittent, the mean value of scintillation variance $\langle\sigma_\chi^2\rangle$ (in dB) can be expressed by the following formula:^{12,22}

$$\langle\sigma_\chi^2\rangle = 42.9G(D_a)k^{7/6} \int_0^L \langle C_n^2(r) \rangle r^{5/6} dr \quad (12)$$

where $G(D_a)$ is the antenna averaging factor, k is the wavelength number and r is the slant path within the turbulent slab of slant thickness L . Note that the ensemble average (indicated by angle brackets) takes into account the local intermittence of the atmospheric turbulence in a statistical way. The mean value of the turbulence structure constant $\langle C_n^2(r) \rangle$ is given by:¹³

$$\langle C_n^2(r) \rangle \cong a^2 L_{oe}^{4/3} F_s(r) \langle M(r) \rangle^2 \quad (13)$$

where $a = 2.8$, L_{oe} is the effective outer scale (approximately 10 m, generally), F_s is the so-called intermittence factor (giving an average index of the local atmospheric instability related to the wind velocity gradient) and $\langle M \rangle$ is the mean vertical refractivity gradient. In practical applications, the ensemble average is estimated through a spatial average within a layer determined by the vertical resolution of the radiosounding so that a layered atmosphere is considered.

In the numerical simulation we have performed, a large database of radiosounding observations (RAOBs) with a vertical spatial resolution of approximately 150 m or smaller, performed at Milan between January 1980 and December 1989, has been examined. An accurate selection of the clear-sky RAOBs has been carried out in order to exclude rainy conditions. For each meteorological profile set (i.e. temperature, pressure, relative humidity and wind vector), the $\langle C_n^2 \rangle$ value at each layer has been derived from equation (13) and the total received scintillation power, i.e. mean variance $\langle\sigma_\chi^2\rangle$, has been calculated through equation (12) for a given fre-

quency, angle and antenna diameter. The turbulence height H (related to L in equation (12)) has been fixed as a function of a humidity density threshold, set to 10^{-3} g/m³ in this work.²² The latter choice stems from the fact that at radiowaves, the scintillations are mainly caused by the humidity variations in the first few km from the ground.²⁰

The output of the above simulation has consisted of approximately 3600 received scintillation powers associated to the ground meteorological measurements, to the vertically averaged structure constant C_n^2 , and to the vertically integrated water vapour content. The reason for focussing on prediction relationships involving only surface meteorological measurements is due, on one hand, to the difficulty sometimes encountered finding a large historical RAOB database at a given site and, on the other hand, to the ease of employing formulae involving only surface variables. By applying the statistical regression analysis to the simulated database on a daily basis and then taking the average of the results over each month, prediction relationships on a monthly basis have been found depending on the regression model function used to relate the input surface variables to the monthly predicted $\overline{\sigma_\chi^2}$ or $\overline{\ln(\sigma_\chi^2)}$. Note that in the following section the overbar will always indicate an average on a monthly basis.

The advantage of the above approach is related to the possibility of choosing the proper meteorological database to recompute the regression coefficients by new numerical simulations, thus saving further costs of setting new propagation experiments. Of course, the results are conditioned to the goodness of the electromagnetic model describing the interaction between microwaves and turbulent atmosphere. Two possible choices of regression formulae have given interesting results and will be described in the following section.

The first model has been called 'Direct physical-statistical prediction' (DPSP). The 'physical' and 'statistical' terms refer to the simulation-based and to the regression-based method, respectively, whereas 'direct' refers to the kind of regression formula used. This model is based on the direct correlation between the monthly average of $\ln(\sigma_\chi^2)$ and T (like the Ortgies-T model in equation (10)), which therefore gives us the μ -parameter if log-normal distribution is assumed (see equation (8)). A fairly high correlation on a monthly basis has also been found between the height H of the turbulent layer, defined as stated previously, and ground temperature data as a result of the corresponding good correlation between ground temperature and humidity.²⁰ Notice that H is usually taken as a fixed value equal to 1000 m or 2000 m,^{16,17} and plays a role in determining the antenna averaging factor by means of the calculation of the first Fresnel-zone radius $\sqrt{\lambda L}$. To take into account the antenna size effect in DPSP, we used the antenna aperture averaging factor formula and the frequency scaling factor

given by the ITU-R (see equations (4) and (5), respectively). The prediction relationship is thus as follows:

$$\overline{\ln(\sigma_\chi^2)} = \ln(G(R_{\text{eff}}; \bar{H}) \cdot \sin^{-2.4\theta} \cdot k^{1.166}) + \overline{\ln(\sigma_{\chi,\text{norm}}^2)} \quad (14)$$

with

$$\overline{\ln(\sigma_{\chi,\text{norm}}^2)} = -15.84 + 0.1235\bar{T} \quad (14a)$$

$$\bar{H} = 2058 + 94.5\bar{T} \quad (14b)$$

where k is the wave number, θ is the elevation angle and the superscripts over H (in m) and T (in °C) indicate monthly averaged values. Note that dependence of the function G on \bar{H} has been written explicitly.

The validity of equation (14b) is related to the climatological region where the radiosounding data were available, i.e. temperate subocenic climate at mid-latitudes with monthly average temperatures \bar{T} between -5°C and 35°C . The comparison of equation (14b) with the analogous quadratic form, given by Rucker and Dintelmann,²⁶ shows some differences: for example, with $\bar{T} = 15^\circ\text{C}$ equation (14b) gives $\bar{H} = 3475$ m, whereas from Reference 26 it results in $\bar{H} = 1888$ m. On the other hand, the value range given by equation (14b) is in a good agreement with the one given by Vilar and Haddon (from 1 up to 5 km).²¹

The second model has been called modelled physical-statistical prediction (MPSP), where the adjective ‘modelled’ refers to the fact that a physical model for the regression formula is used. In particular, if a thin layer of homogeneous turbulent atmosphere (characterized by a thickness and a base height) is assumed, equation (12) can be solved analytically, giving a simple formula to derive scintillation variance and layer parameters.^{7,14,21} The formulation of the model derives from the high correlation on a monthly basis between the logarithm of the vertically averaged structure constant $\ln(C_n^2)$ and the surface temperature \bar{T} and from the approximation of the thickness of the layer by $(\bar{H} 400/2000)$. In the latter expression, 400 m and 2000 m are the common values for the thin layer thickness and the slab height, respectively. The antenna aperture averaging factor formula is that of the ITU-R (see equation (5)), whereas the frequency scaling factor is consistent with Tatarskii’s theory. The final relationship for MPSP is as follows:

$$\overline{\ln(\sigma_\chi^2)} = \ln \left(G(R_{\text{eff}}; \bar{H}) \cdot 42.25 \cdot k^{7/6} \cdot \left[\frac{\bar{H}}{\sin\theta} \right]^{5/6} \cdot \frac{400}{2000} \frac{\bar{H}}{\sin\theta} \right) + \overline{\ln(C_n^2)} \quad (15)$$

with

$$\overline{\ln(C_n^2)} = -31.87 + 0.0684\bar{T} \quad (15a)$$

where \bar{H} is given by equation (14b) and the factor $(\bar{H} 400/2000)$ can be interpreted as the effective thickness of a thin turbulent layer with the bottom level at altitude \bar{H} .

The previous formulae need only surface temperature \bar{T} as an input parameter. In a more extensive work, we also investigated another version of this model using \bar{T} and the monthly vertically integrated water vapour content (VIWVC) as input parameters. It is worth noting that VIWVC would be predictable with a good accuracy by using a dual-channel ground-based microwave radiometer, i.e. from the measured brightness temperature at 20.6 GHz band and 31.6 GHz band.⁴ The correlations obtained using \bar{T} and VIWVC as input parameters are usually stronger than by using only \bar{T} , so that the model should therefore be more accurate. When using the VIWVC as a statistical predictor, a correlation between σ_χ and VIWVC stronger than that between $\ln(\sigma_\chi^2)$ and VIWVC has been found, thus obtaining σ_χ instead of μ . Similarly, a stronger correlation between \bar{H} and $\ln(\text{VIWVC})$ has been found than between \bar{H} and VIWVC. Unfortunately, the lack of corresponding radiometric measurements did not allow us to check the version of those models using the VIWVC and \bar{T} as inputs.

For σ_χ^2 we assumed a log-normal PDF and because the PDF followed by $p(\chi|\sigma_\chi^2)$ is generally assumed to be Gaussian, the $p(\chi)$ can be estimated by numerically integrating the PDF product (see equation (1)).¹¹ Using the complementary error function (ERFC), we give the following result for the case of signal enhancement, which is symmetric with respect to the fading signal:

$$p(\chi \geq \chi_o) = \int_0^\infty \frac{1}{\sqrt{2\pi} \cdot s \cdot \sigma_\chi} \cdot \text{ERFC} \left(\frac{\chi_o}{\sqrt{2}\sigma_\chi} \right) \cdot \exp \left(-\frac{(\ln\sigma_\chi^2 - \mu)^2}{2s^2} \right) d\sigma_\chi \quad (16a)$$

$$p(\chi \geq \chi_o) = p(\chi \leq -\chi_o) \quad (16b)$$

The last equation (16b) holds because of the symmetry property of the Gaussian function assumed for the short-term log-amplitude fluctuations.

In the next sections, we will compare the above DPSP and MPSP models with *Olympus* measurements, setting the value of $\mu = \ln(\sigma_\chi^2)$ as given by equations (14) and (15). Because the parameter $s = \sigma_{\ln(\sigma_\chi^2)}$ is needed to specify equation (16a), we have computed its value from our simulated database on a monthly basis, getting values from 0.75 (winter time) to 1.20 (summer time). These values are in fairly good agreement with the range of s values derived by Ortgies, who proposed an s mean value of 1.01. Moreover, the mean value proposed by Ortgies is consistent with our own experimental results (see Section 4) that provide an average s

value of 0.92. In the next section, we will set the s value to the Ortgies value of 1.01 because it has been tested over a large set of satellite measurements.

3. OLYMPUS AND GROUND METEOROLOGICAL DATA

3.1. Beacon sites and data processing

The experimental data used in this work have been taken during the year 1992 at the two groundstations of Louvain-la-Neuve (Belgium) and Milan (Italy) along the down-link of the Olympus satellite, designed and launched in 1989 by the European Space Agency (ESA). Table I shows the characteristics of the beacons studied.

Louvain-la-Neuve data. Twelve months of Olympus data have been available from 1 January 1992 to 31 December 1992 at 12.5 GHz, and 10 months at 29.7 GHz from 1 January 1992 to 31 October 1992, both acquired at a sampling rate of 1 Hz.^{6,26} Because the Louvain-la-Neuve (LLN) groundstation was not equipped with a tracking system, the pre-processing procedure to remove errors caused by satellite movements has been carried out manually.

A clear-sky threshold of -1 dB has been applied to the log-amplitude time series. A further threshold has also been imposed on scintillation data because of the noise of the equipment, so that only periods with scintillation variances greater than 0.46×10^{-3} dB² (at 12.5 GHz) and 1.96×10^{-3} dB² (at 30 GHz) have been considered as scintillation events. A low-pass filtering, consisting of a moving-average window of 61 s length has been then applied, computing for each second the mean value and the variance of log-amplitude scintillations.

Table I. Specifications of earth stations at Olympus beacons in Louvain-La-Neuve and Milan

Characteristics of the earth station	Louvain-la-Neuve Microwaves Laboratory UCL (Belgium)	Milan Politecnico (Italy)
Position:		
• latitude	50°13' N	45.5° N
• longitude	5°15' E	9.2° E
• altitude	162 m	25 m
Beacon's frequency	12.5 GHz/29.7 GHz	19.77 GHz
Antenna's diameter	1.8 m	1.5 m
Antenna's elevation angle	27.6°	30.6°
Post-processing sampling rate	1 Hz	1 Hz

Milan data. Five months of Olympus data have been available from 1 July 1992 to 6 December 1992 at 19.77 GHz, acquired at a sampling rate of 1 Hz.¹⁷ As a result of the lack of a tracking system and in order to separate the influence of the movement of the satellite, data have first been corrected by subtracting the Fourier components of period 3, 6, 12 and 24 h.

A clear-sky threshold of -1.5 dB has been applied to the log-amplitude time series in order to select clear-air events. Thereafter, the Olympus signal has been filtered for rain attenuation studies by using a low-pass filter with a cut-off frequency of 0.01 Hz, and for scintillation studies by applying a fifth-order Butterworth high-pass filter with a cut-off frequency at -3 dB of 0.008 Hz.¹¹ The cut-off frequency is slightly higher than the one used elsewhere (approximately 0.004 Hz)⁹ and this is because of the need to avoid spurious low frequency components due to satellite periodic movements mentioned above. From the spectral analysis of the Milan Olympus data, it can be concluded that only a few percent of scintillation power has been lost by choosing 0.008 Hz cut-off frequency. All the computed values of scintillation log-amplitude and variance have then been resampled every minute for recording.

The main differences between LLN and Milan data are basically caused by differences of local climatology, beacon frequencies and antenna sizes. For Louvain-la-Neuve data, the application of a threshold on variance data can explain the fact that the small values of scintillation variance occur only approximately 1 per cent of the time. For Milan data, no threshold has been applied because of the lack of information concerning the noise of the equipment.

3.2. Ground meteorological measurements

At Louvain-la-Neuve, the meteorological data have been provided as daily mean values of temperature and relative humidity. In order to select clear-sky data, only measurements with cumulative precipitation under 0.1 mm have been kept.

At Milan, the meteorological data, consisting of surface temperature and relative humidity, were measured every 10 min. Only the meteorological measurements corresponding to the clear-sky threshold applied on the log-amplitude measured from the satellite have been retained. In the Milan data set, we thus have a correspondence between Olympus measurements and surface meteorological data every 10 min. Figure 1 shows a three-dimensional plot of mean scintillation intensity as a function of mean surface temperature and month index, confirming that the worst months characterized by high scintillation variance are the mid-summer ones (July and August) and the worst hours are the ones around 2 p.m. Similar three-dimensional plots of surface temperature, relative humidity and wet

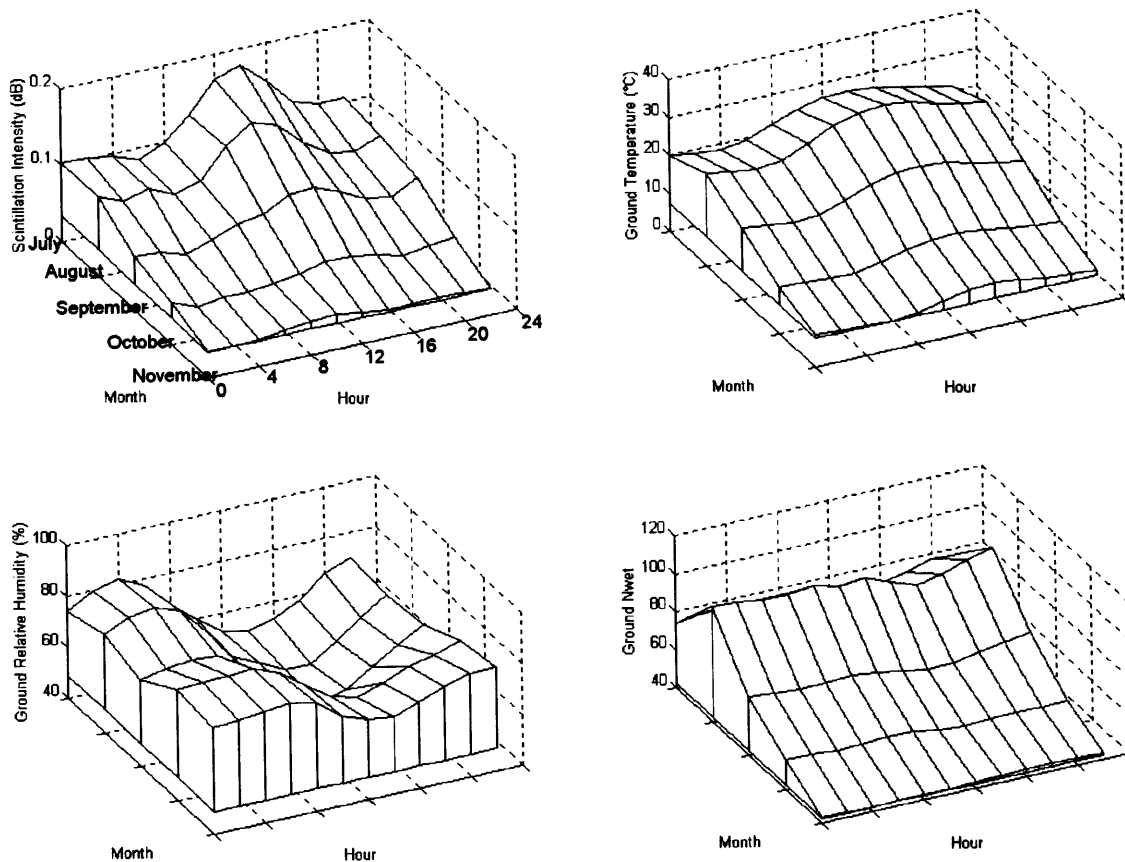


Figure 1. Diurnal and seasonal variation of 19.77 GHz Olympus scintillation intensity (top-left panel), ground temperature (top-right panel), ground relative humidity (bottom-left) and ground wet refractive index N_{wet} (bottom-right) from July to November 1992 as measured at the Milan station

refractivity (N_{wet}) are also shown in the figure. The fairly good positive correlation between scintillation intensity and ground temperature and the negative correlation between scintillation intensity and ground relative humidity is apparent, a result already reported in the literature.²⁰

As already stated, a common choice is to assume the effective turbulence height \bar{H} equal to 1000 m or 2000 m.^{16,17} Figure 2 shows, in the left panel, the yearly evolution of the effective height \bar{H} as derived from Milan radiosoundings during 1980, fixing a humidity threshold (see Section 2), as computed from through equation (14b), and as imposed using a fixed value of 2000 m. Correspondingly, on the right panel, the antenna averaging factor G given by equation (3) is also shown using the three ways of determining \bar{H} illustrated in the left panel. The underestimation of G by using a fixed height of 2000 m through the year is less than 2 per cent (up to 8 per cent when choosing $\bar{H} = 1000$ m), but the impact of \bar{H} on prediction accuracy can be much stronger because it can be explicitly present in variance estimation formulae (as in equation (15)).

4. INTERCOMPARISON OF PREDICTION MODELS

Before applying each statistical model to Olympus and meteorological data sets previously described,

we have checked some of the assumptions made in the prediction models studied. To this aim, we have used only the Olympus scintillation data at 19.77 GHz measured from July to November 1992 in Milan.

4.1. Scintillation variance estimate from meteorological measurements

Best-fitting cumulative distribution. A well established hypothesis coming from theory and experimentation^{10,16} is that the log-amplitude fluctuations, i.e. $p(\chi|\sigma_\chi)$, follows a Gaussian distribution in the short term. The problem of the PDF $p(\sigma_\chi)$ followed by σ_χ in the long term is more debated. For example, Karasawa and the ITU-R models assume a Gamma PDF distribution for σ_χ , Ortgies model supposes a log-normal PDF for σ_χ^2 and others²² use the Rice-Nagakami for σ_χ^2 . In this test, we have tried all of them, also considering the Rayleigh and the exponential distributions due to the analogy between scintillation and noise process.

Figure 3 shows the comparison of the previous PDF with that measured at Milan in terms of cumulative distribution functions. Table II lists the parameters of each PDF as derived from Olympus measurements in order to ensure the best fit. According to this figure the log-normal distribution is the best-fitted PDF for the long-term variation of σ_χ^2 . It

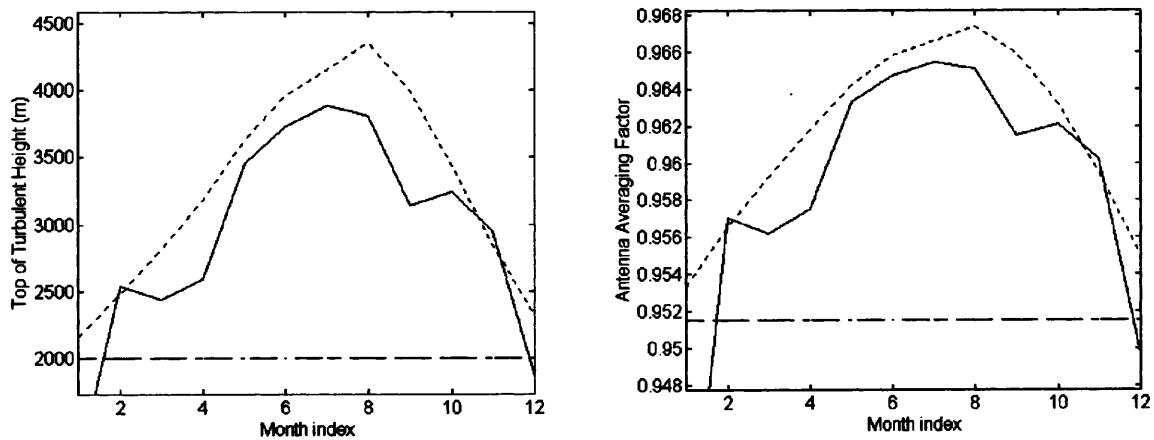


Figure 2. (Left panel) Effective height H of turbulent atmosphere as a function of month index, numbered from 1 (January) to 12 (December), derived from Milan radiosounding humidity profiles in 1980 (solid line), from the prediction formula given by equation (14b) (dotted line) and a fixed value equal to 2000 m (dashed line). (Right panel) Antenna aperture averaging factor G given in equation (3) as a function of month index, numbered from 1 (January) to 12 (December), computed by using effective height H derived from Milan radiosoundings humidity profiles in 1980 (solid line), from the prediction formula given by equation (14b) (dotted line) and from a fixed value equal to 2000 m (dashed line)

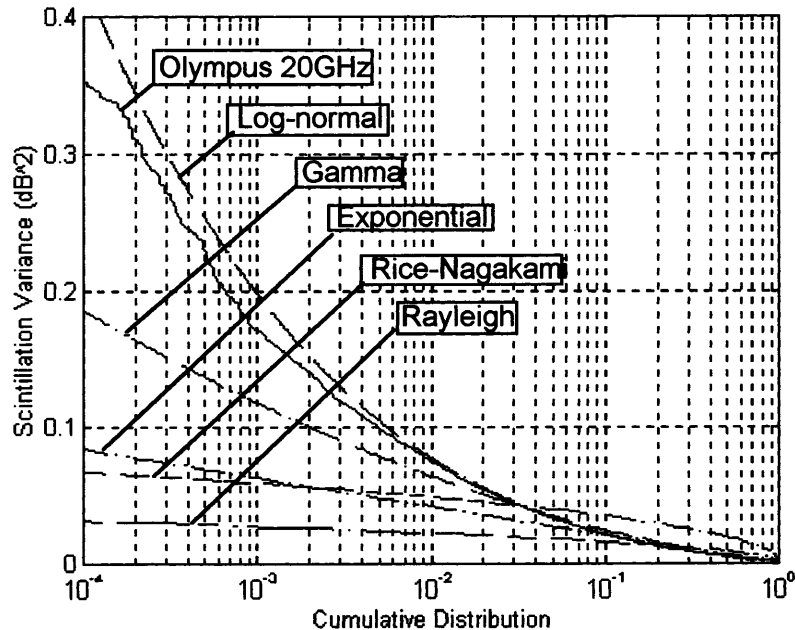


Figure 3. Bestfitting cumulative distributions of scintillation variance, derived by imposing the statistical parameters listed in Table II, and compared with Olympus measurements (solid line) at 19.77 GHz at Milan from July to November, 1992. The log-normal, the Gamma, the exponential, the Rayleigh and the Rice–Nagakami probability density functions are shown

Table II. Statistical parameters of fitted PDF using Olympus Milan data at 19.77 GHz

Best-fitted probability density function	Parameters	First parameter value	Second parameter value
Gaussian	m, σ	0.0091	0.0174
Log-normal	μ, s	-5.46	1.23
Gamma	α, β	2.36	29.58
Rayleigh	λ	0.0073	
Exponential	m	0.0091	

also appears that the Gamma distribution significantly underpredicts the high values of the scintillation intensity. To some extent, these results were expected because Gamma PDF has proved to be suitable for low elevation angles and humid areas, producing strong scintillations, whereas log-normal distribution is adequate for high elevation angles and continental regions, such as the Milan and LLN sites.

Mean value of scintillation variance. The analysed prediction models propose various relations linking the parameters of their assumed PDF to ground measurements. Because Ortgies models and

DPSP and MPSP models give the estimate of the log-normal parameter μ , in order to show the results in a more readable way, we have converted μ in the mean variance scale by using²⁵ $\overline{\sigma_x^2} = \exp(\mu + 0.5 s^2)$ with s specified by the model itself. The Karasawa and ITU-R will be shown separately in terms of scintillation mean intensity.

Figures 4a and 4b show the predictions given by the models using surface Nwet as the input parameter, i.e. on the one hand, the Karasawa and ITU-R models and, on the other, the Ortgies-N model. The ITU-R model tends generally to overestimate the mean intensity σ_x , especially for small Nwet values. The Karasawa model gives a closer agreement with measurements on average, even though an overestimation results for smaller values of Nwet. The prediction given by the Ortgies-N model seems fairly accurate up to 80 per cent of Nwet, but tends to diverge for higher Nwet values.

Figure 5 show the same predictions as in the previous figure, but for the models using surface temperature T as the input parameters, i.e. DPSP, MPSP, and Ortgies-T models. The relationship proposed by Ortgies using the ground temperature seems to underestimate $\overline{\sigma_x^2}$ values for large T values. The DPSP and MPSP models both seem to be in

fairly good agreement with measured $\overline{\sigma_x^2}$, even though DPSP tends to overestimate $\overline{\sigma_x^2}$ for temperatures greater than 20°C. The latter result confirms the potential of the DPSP and MPSP approach and the advantage to train the model function numerically on the appropriate climatological data set. Note that the Olympus data referred to a period which was not included in the historical radiosounding set used to derive MPSP and DPSP regression coefficients. Moreover, the accuracy of the PSP method of prediction strongly depends on the turbulent atmosphere model used (using equation (13), intermittence effects have also been included in the numerical simulations) and on the chosen regression model function.

Standard deviation of scintillation variance. By using the available Olympus measurements, we have found a ratio R between the square of its mean value $\overline{\sigma_x^2}$ and the variance of σ_x^2 , i.e.:

$$R = \overline{\sigma_x^2} / \sigma_x^2 \quad (17)$$

ranging from 2.78 to 6.39, and a mean ratio equal to 4.27. The quantitative results are listed in Table III for the Milan site on a monthly basis.

Both the Karasawa and ITU-R models assume a ratio R equal to 10 (see equation (6)) which is much higher than the one derived in this case study. This high value of R might explain the significant underestimation of log-amplitude probability when using the above prediction models (see Figure 10 in the next Section).

The Ortgies models assume that the value of the parameter s of the log-normal PDF, given in equation (8), (also used in the DPSP and MPSP models) ranges from 0.85 to 1.15 and its mean value is equal to 1.01. From the Olympus measurements, we have found values ranging from 0.69 to 1.12, with a mean value of 0.92, which is slightly lower than the one given by Ortgies.

4.2. Long-term prediction on monthly and yearly basis

So far the different assumptions made in each prediction model have been analysed and tested separately. In this section, we have applied the prediction models as they are proposed directly to monthly averaged ground meteorological measurements of the Milan and LLN sites, and show the results in terms of cumulative distribution functions. Note that we show all the results in terms of scintillation variance, converting the scintillation intensity predictions (Karasawa and ITU-R) by means of the discretization of the associated cumulative distribution functions (CDF) and making the discrete probability sum.

Cumulative distribution of scintillation variance. Figures 6a, 6b and 6c compare the cumulat-

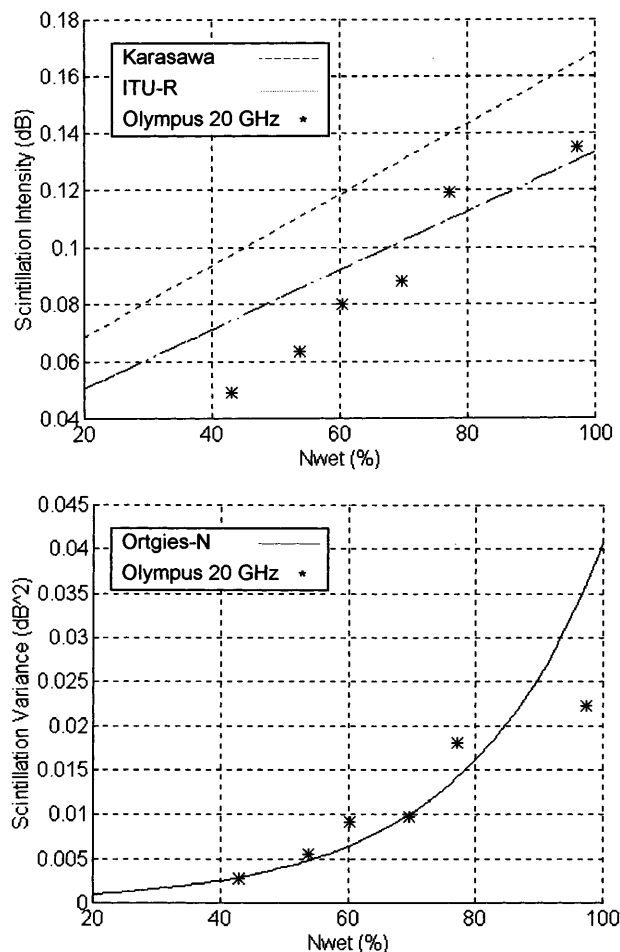


Figure 4. (a) Karasawa and ITU-R predictions of mean scintillation variance against Nwet compared with Olympus monthly mean values at 19.77 GHz from July to November, 1992 at Milan. (b) Same as (a), but for Ortgies-N predictions

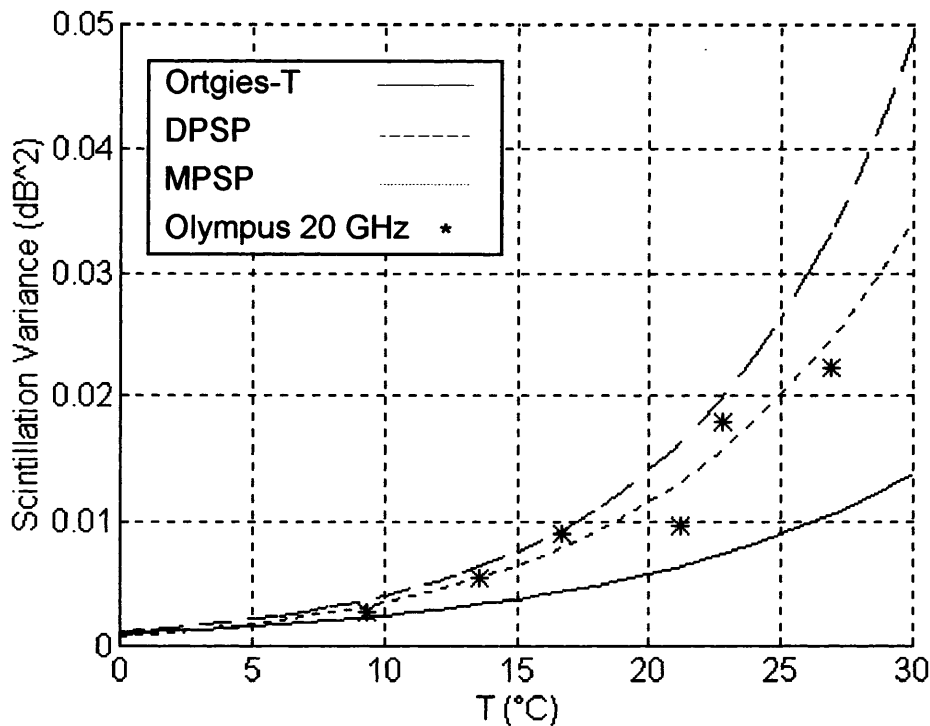


Figure 5. Ortgies-T, DPSP and MPSP predictions of mean scintillation variance against surface temperature T and compared with Olympus monthly mean values at 19.77 GHz from July to November, 1992 at Milan

Table III. Ratio R , defined in equation (17), derived from Milan data at 19.77 GHz on a monthly basis

Month of 1992	Ratio R at 20 GHz
July	3.83
August	4.49
September	3.89
October	2.78
November	6.39

ive distribution of σ_χ^2 resulting from DPSP, MPSP, Ortgies-T, Ortgies-N models when using beacon data at 12.5 GHz in LLN; at 20 GHz at Milan and at 30 GHz in LLN, respectively. Each figure consists of four panels where, on a monthly basis, the results for the worst-case months (July and August) are plotted; the solid line always represents the Olympus measurements in all three figures.

The analysis of these figures shows that the Ortgies-T model always underestimates the high values of scintillation, whereas the Ortgies-N model is fairly accurate even though it tends to overestimate scintillation in August when the wet refractivity is higher. The DPSP and MPSP models give a fairly accurate prediction of scintillation variance, with a trend towards underestimating relatively strong scintillation at 29.7 GHz, and DPSP variances generally being higher than MPSP variances. On average, it is the MPSP model which shows the best results for all the three beacons.

Figure 7 shows the same plots as in Figure 6b for the Milan site at 19.77 GHz, but applying the

Karasawa and ITU-R models (plots similar to Figure 6a and 6c are not shown for the sake of brevity). The top panels refer to the results obtained by directly applying the two models and show a significant underprediction for all the probability values. This is not surprising because we have already found that using a Gamma instead of a log-normal distribution leads to the underprediction of high scintillation values. Moreover, it has also been shown that the assumed relationship between $\overline{\sigma_\chi}$ and σ_{σ_χ} (i.e. the ratio R given by equation (17)) underestimates the values of σ_{σ_χ} with respect to the available measurements.

The latter consideration and its impact on the final results has been checked as follows. We have replaced the value of σ_{σ_χ} with the measured value of σ_{σ_χ} as derived from our Olympus data (see Table III). The bottom panels of Figure 7 show the same plots as in the top panels but after modifying the ITU-R and Karasawa models, and demonstrate that the agreement with measurements is strongly increased. This result can lead to the conclusion that the models of Karasawa and ITU-R are not well fitted to the meteorological conditions, and partly, to beacon specifications analysed in this work. In fact, the Karasawa model was set up by using a beacon with low frequencies, very low elevation angles, large antennae, and moreover in a very different type of climate.¹⁶

In order to apply the above prediction models, created with monthly averaged variables, to periods longer than a month (e.g. a year), we have to apply a probability sum of monthly predictions. In fact,

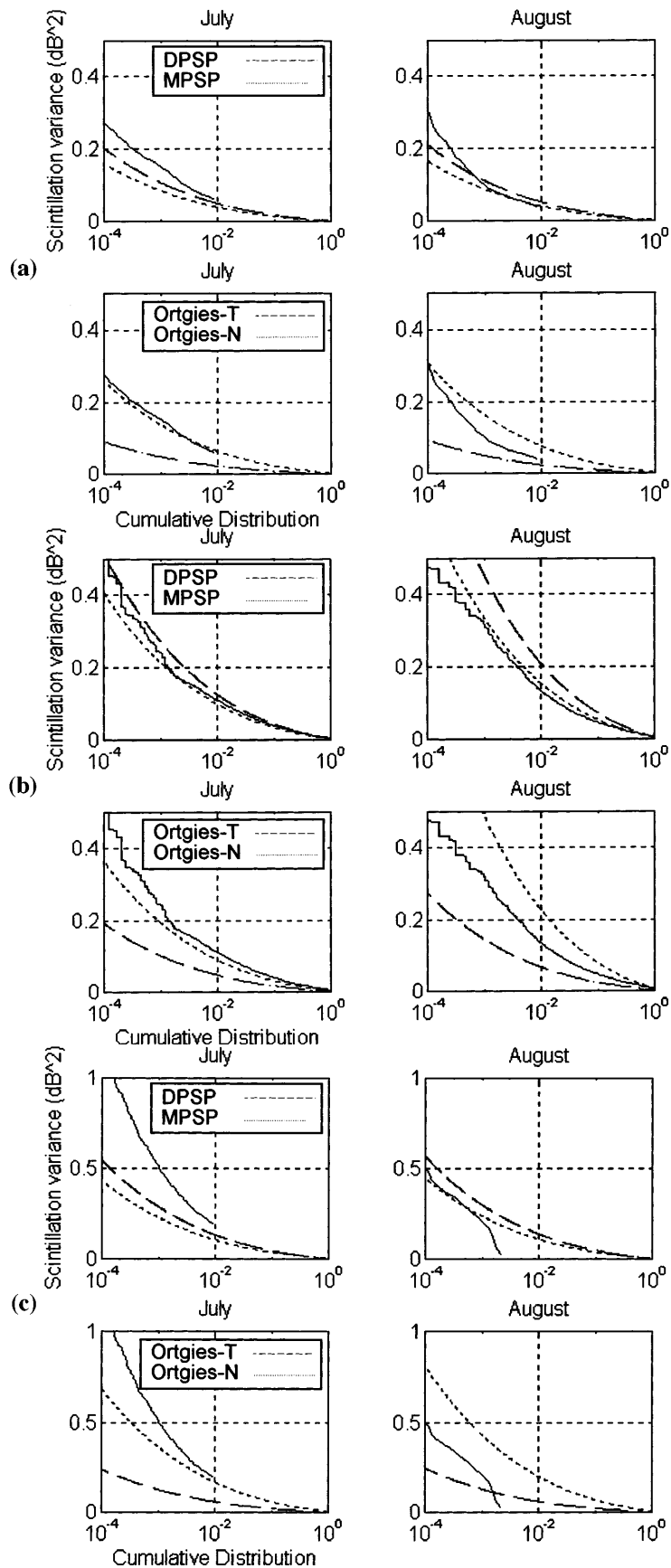


Figure 6. (a) (Top panels) DPSP and MPSP predictions of cumulative distribution of scintillation variance compared with Olympus measurements (solid line) at 12.5 GHz at Louvain-la-Neuve during July (right panel) and August (left panel), 1992. (Bottom panels) Same as in top panels, but for Ortgies-T and Ortgies-N. (b) (Top panels) DPSP and MPSP predictions of cumulative distribution of scintillation variance compared with Olympus measurements (solid line) at 19.77 GHz at Milan during July (right panel) and August (left panel), 1992. (Bottom panels) Same as in top panels, but for Ortgies-T and Ortgies-N. (c) (Top panels) DPSP and MPSP predictions of cumulative distribution of scintillation variance compared with Olympus measurements (solid line) at 29.7 GHz at Louvain-la-Neuve during July (right panel) and August (left panel), 1992. (Bottom panels) Same as in top panels, but for Ortgies-T and Ortgies-N

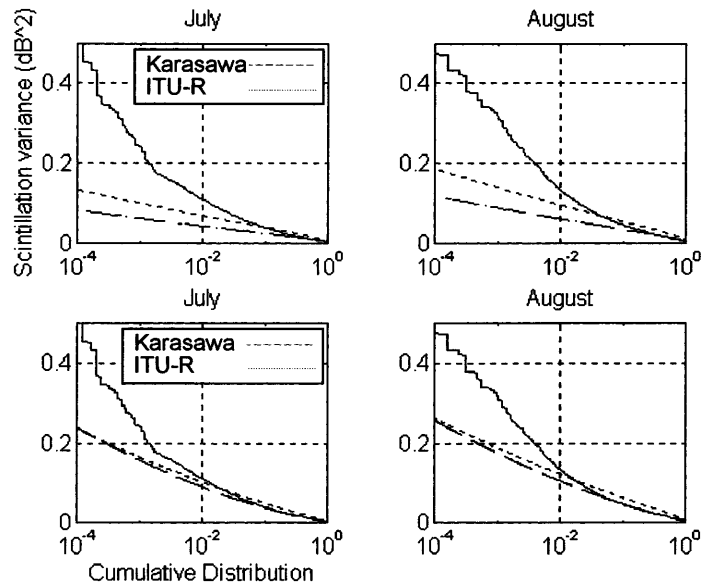


Figure 7. (Top panels) Karasawa and ITU-R predictions of cumulative distribution of scintillation variance compared with Olympus measurements (solid line) at 19.77 GHz at Milan during July (right panel) and August (left panel), 1992. (Bottom panels) Karasawa and ITU-R predictions of cumulative distribution of scintillation variance, modified by applying the measured ratio R and compared with Ortgies-N predictions and Olympus measurements (solid line) at 19.77 GHz at Milan for July 1992

by simply applying the methods with input variables averaged over a year ('average procedure'), it would result in an underestimation of the high values of σ_χ^2 probability because of the smoothing of ground parameter values. On a yearly basis, it is thus necessary to compute scintillation variance probability for each month, sum the probabilities over all the months, and normalize it in order to ensure the unitary normalization of the PDF ('cumulative procedure').

Figures 8a, 8b and 8c show the yearly basis results for DPSP and MPSP, Ortgies-T and Ortgies-N, Karasawa and ITU-R models, respectively, using the above-mentioned 'cumulative procedure' for the Milan site only at 19.77 GHz. Comments on this figure are almost the same as for Figures 6 and 7. Note that the Karasawa and ITU-R models have not been corrected as done in the bottom panels of Figure 7.

Figure 9 shows the difference between the results given by the 'average' and 'cumulative' procedures in the case of the Ortgies-N model for the LLN site at 12.5 GHz. As expected, the results given by using the 'cumulative procedure' are in a better agreement with measurements than by applying the 'average procedure'.

Cumulative distribution of scintillation log-amplitude. As explained in Section 2, in Karasawa and ITU-R models the log-amplitude χ is divided into two parts, the fluctuation signal 'enhancement' and the 'fading' (see equations (7a) and (7b)). The Ortgies-N, DPSP and MPSP log-amplitude prediction has been computed by numerical integration of the formula given in equation (16a), resulting in an equal probability of signal fading and enhancement (see equation (16b)). We have tested all the predic-

tion models for the monthly prediction of the cumulative distribution of χ in case of strong scintillation, weak scintillation, and for periods longer than one month, even though we illustrate only the worst-month case.

Figure 10 shows the results for scintillation log-amplitude fading (top panel) and enhancement (bottom panel) prediction, using the Karasawa and ITU-R models for the worst month (i.e. July 1992) at Milan at 19.77 GHz. Figure 11 shows the amplitude fluctuation prediction (without distinguishing between fading and enhancement) for the same month and beacon as in Figure 10, but for DPSP and MPSP models (top panel) and the Ortgies-T and Ortgies-N models (bottom panel). The Olympus-measured cumulative distribution of the signal amplitude fluctuations is also shown by a solid line and divided into an enhancement and a fading component only in Figure 10.

From Figure 10, as expected, the Olympus signal fluctuation fading is higher than that of the enhancement. The measured cumulative distribution for small χ seems to present a concavity showing a behaviour similar to that also found in other Olympus sites.⁶ Both the Karasawa and ITU-R models seem to overestimate small values of log-amplitude fluctuations corresponding to a high percentage of time (>1 per cent). For relatively high scintillation values (>0.5 dB), the ITU-R model shows a better agreement between enhancement/fading prediction and Olympus measurements with respect to the Karasawa model. The prediction models shown in Figure 11 do not allow the discrimination of fading and enhancement components. Again, all the prediction results tend to overestimate the amplitude fluctuations for a given probability. The Ortgies-N, DPSP and MPSP prediction models are in fairly

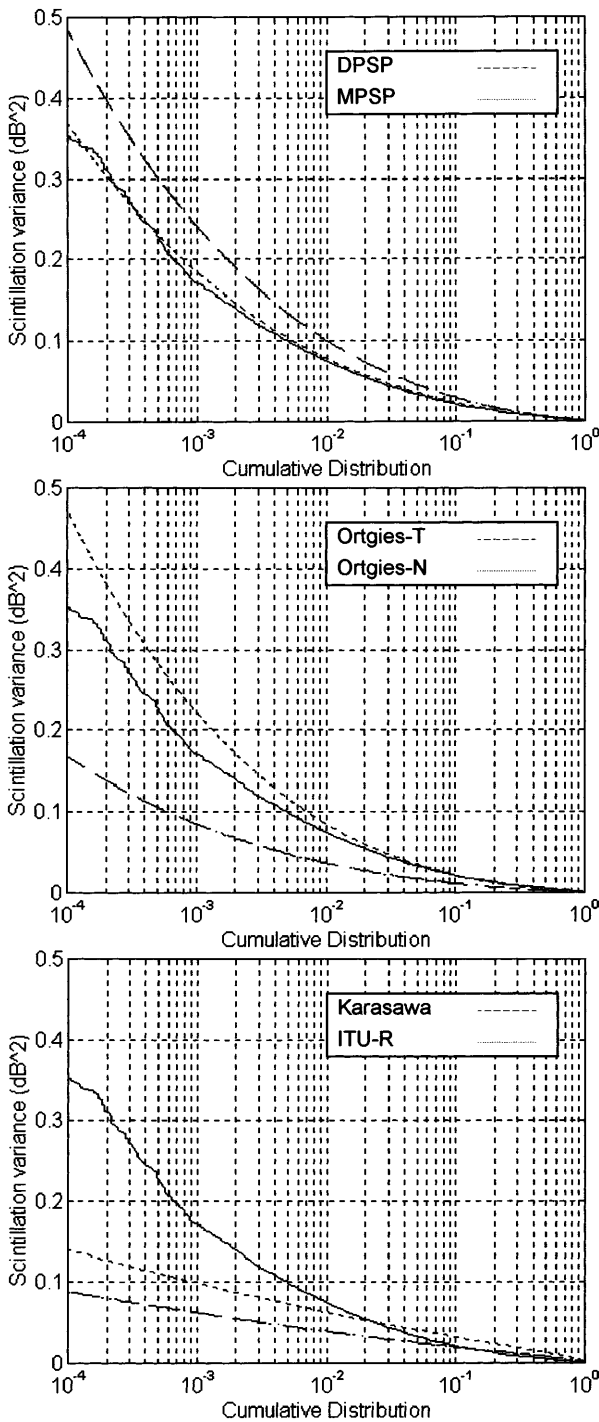


Figure 8. (a) DPSP and MPSP predictions of cumulative distribution of scintillation variance compared with Olympus measurements (solid line) at 19.77 GHz at Milan on a yearly basis (using the available months of 1992). (b) Same as in Figure 8(a), but for Ortgies-T and Ortgies-N predictions. (c) Same as in Figure 8(a), but for Karasawa and ITU-R and in terms of scintillation intensity

good agreement with the Olympus measurements for probability values less than 0.005, i.e. signal fluctuation greater than 0.5 dB; for smaller fluctuation values, a discrepancy comparable to the one noticed when using the Karasawa and ITU-R models is found.

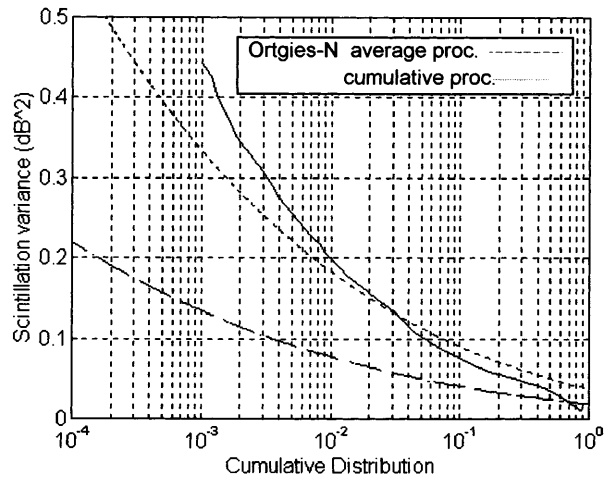


Figure 9. Ortgies-N predictions of cumulative distribution of scintillation variance compared with Olympus measurements at 12.5 GHz at Louvain-la-Neuve for the whole year 1992, showing the different results obtained by using the 'average procedure' and the 'cumulative procedure'

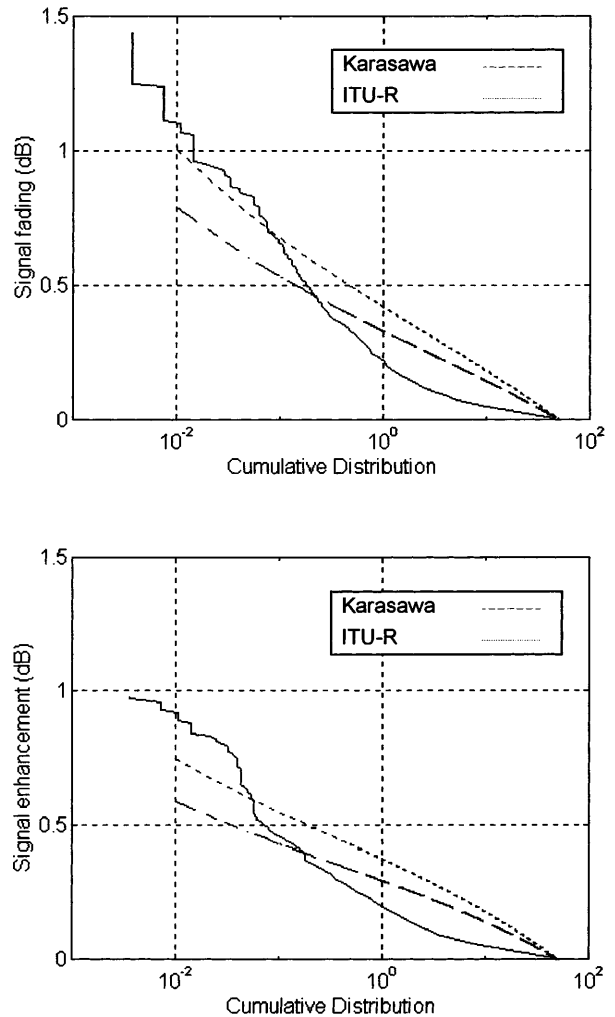


Figure 10. (Top panels) Karasawa and ITU-R predictions of scintillation log-amplitude fading compared with corresponding Olympus measurements (solid line) at 19.77 GHz at Milan for July 1992. (Bottom panels) Same as in top panels, but for scintillation log-amplitude enhancement

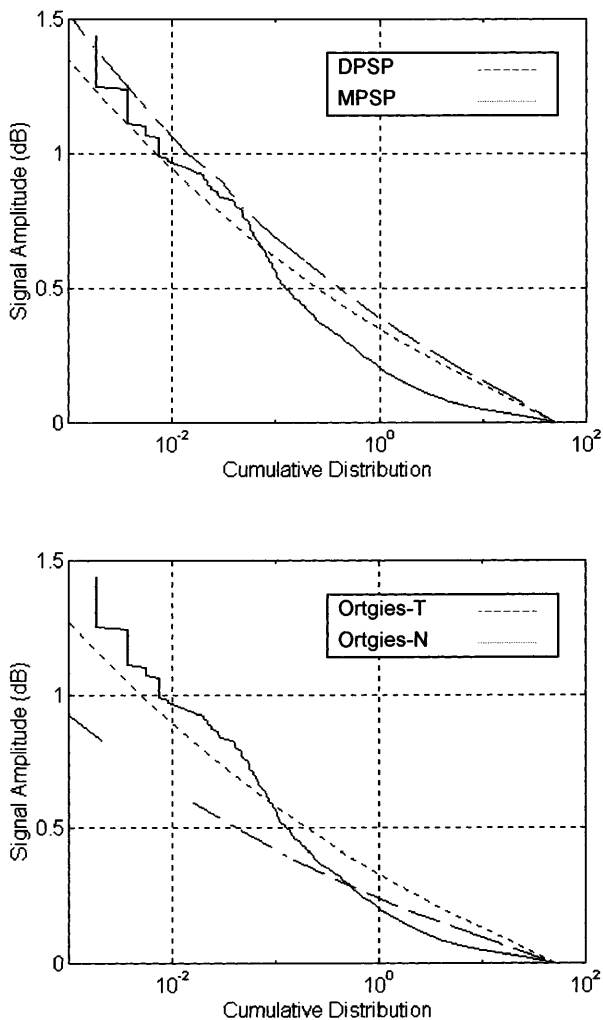


Figure 11. (Top panels) DPSP and MPSP predictions of mean scintillation log-amplitude compared with Olympus measurements (solid line) at 19.77 GHz at Milan for July 1992. (Bottom panels) Same as in top panels, but for Ortgies-T and Ortgies-N predictions

5. CONCLUSIONS

In this study, we have compared the scintillation prediction derived from the statistical models of Karasawa, ITU-R and Ortgies, as well as from two new statistical models, the direct and the modelled physical-statistical prediction, which have been presented here.

After having checked the various assumptions of each model and comparing them globally with Olympus measurements, we can conclude that for our data and in our conditions: (i) the log-normal PDF seems to be the best fitted PDF for long-term variations of the scintillation variance; (ii) the model proposed by Ortgies, and the two new models can give fairly accurate predictions of the cumulative distribution of scintillation variance; (iii) Karasawa and ITU-R prediction models seem less fitted to the conditions of our case study, but their estimation improved when using statistical parameters experimentally tuned; (iv) the scintillation variance model results are also applicable for the prediction of scintillation log-amplitude, if the mean and standard

deviation of scintillation intensity is properly estimated; (v) in case of intense scintillation, the assumed symmetrical PDF of log-amplitude scintillation is not generally adequate to explain the enhancement and fading of measured scintillation amplitude.

The introduction of new parameters within the prediction models, such as the effective height of the turbulent atmosphere and the structure constant C_n^2 , predicted directly from ground measurements, as well as the use of a parametrized formula for the antenna aperture factor, might represent an improvement of existing estimation methods. An interesting perspective would also be the inclusion into the prediction models of a larger set of input parameters, such as the vertically integrated water vapour content, estimated from measurements of ground-based microwave radiometers.

ACKNOWLEDGEMENTS

We are grateful to P. Basili and P. Ciotti for their helpful advice and to one of the reviewers whose comments greatly improved the readability and consistency of the paper. H. Vasseur and I. Adams helped in collecting LLN data. We acknowledge Fondazione Ugo Bordoni (Rome, Italy) that provided the Milan radiosounding set. This work has been partly supported by Italian Ministry of Scientific and Technology Research (MURST) and Agenzia Spaziale Italiana (ASI). The Erasmus programme of the European Union allowed one of the authors (G.P.) to carry out most of the work at the University 'La Sapienza' of Rome.

REFERENCES

1. O. P. Banjo and E. Vilar, 'Measurements and modeling of amplitude scintillations on low-elevation Earth-space paths and impact on communication systems', *IEEE Trans. Commun.*, **34**, 774-780 (1986).
2. P. A. Watson and Y. F. Hu, 'Prediction of attenuation on satellite-earth links for systems operating with low fade margins', *IEE Proc - Microwave Ant. Propag.*, **141**, 467-472 (1994).
3. J. Haddon and E. Vilar, 'Scattering induced microwave scintillations from clear air and rain on Earth space paths and the influence of antenna aperture', *IEEE Ant. Propag.*, **34**, 646-657 (1986).
4. P. Basili, P. Ciotti, G. d'Auria, P. Ferrazzoli and D. Solimini, 'Case study of intense scintillation events on the OTS path', *IEEE Trans. Ant. Propag.*, **38**, 107-113 (1990).
5. E. Matricciani, 'Physical-mathematical model of the dynamics of rain attenuation with application to power spectrum', *Electron. Lett.*, **30**, 522-524 (1994).
6. D. Vanhoenacker, G. Brussard, F. Haidara, G. Ortgies, A. Paraboni, T. Pratt, C. Riva, J. Tervonen, S. Touw and H. Vasseur, 'Atmospheric scintillation', *OPEX Second Workshop, Vol. 1: Reference Book on Attenuation Measurement and Prediction*, (D. Vanhoenacker and J. P. V. Poiars Baptista, eds), Nordwijk, 1994, pp. 49-64.
7. V. I. Tatarskii, *The Effects of the Turbulent Atmosphere on Wave Propagation*, Israel Program for Scientific Translations, Jerusalem, 1971.
8. Y. Karasawa, K. Yasukawa and M. Yamada, 'Tropospheric scintillation in the 14/11 GHz bands on Earth-space paths with low elevation angles', *IEEE Trans. Ant. Propag.*, **36**, 563-569 (1988).
9. Y. Karasawa and T. Matsudo, 'Characteristics of fading on

- low-elevation angle on Earth-space paths with concurrent rain attenuation and scintillation', *IEEE Trans. Ant. Propag.*, **39**, 657-671 (1991).
10. T. J. Mouldsley and E. Vilar, 'Experimental and theoretical statistics of microwave amplitudes scintillation on satellite down-links', *IEEE Trans. Ant. Propag.*, **30**, 1099-1106 (1982).
 11. A. Paraboni, C. Riva, D. Vanhoenacker and H. Vasseur, 'Extraction of scintillations from signal affected by rain', *Proc. 21st Meeting of Olympus Propagation Experiment (OPEX)*, Louvain-La-Neuve (B), 1994, pp. 166-172.
 12. V. I. Tatarskii and V. U. Zavorotni, 'Wave propagation in random media with fluctuating turbulent parameters', *J. Opt. Soc. Am. A*, **2**, 2069-2076 (1985).
 13. G. d'Auria, F. S. Marzano and U. Merlo, 'Model for estimating the refractive-index structure constant in clear-air intermittent turbulence', *Appl. Optics*, **32**, 2674-2680 (1993).
 14. P. Basili, P. Ciotti, G. d'Auria, E. Fionda, U. Merlo, P. Ferrazzoli, D. Solimini and J. Wang, 'Results from studies on scintillation based on the SIRIO experiment', *Alta Frequenza*, **56**, 69-77 (1987).
 15. G. De Angelis, A. Paraboni, C. Riva, F. Zaccarini, G. Dellagiacomma, L. Ordano, R. Polonio, M. Mauri and A. Pawlina, 'Attenuation and scintillation statistics with Olympus and Italsat satellites in Italy', *Alta Frequenza*, **6**, 66-69 (1994).
 16. Y. Karasawa, M. Yamada and J. E. Allnutt, 'A new prediction method for tropospheric scintillation on earth-space paths', *IEEE Trans. Ant. Propag.*, **36**, 1608-1614 (1988).
 17. ITU-R, Report 718-3, 'Effects of tropospheric refraction on radio-wave propagation', *Reports of the CCIR on Propagation in Non-ionized Media*, Annex to Vol. V, Geneva (CH), 1990, pp. 172-176.
 18. G. Ortgies, 'Prediction of slant-path amplitude scintillation from meteorological parameters', *Proc. Int. Symp. Radio Propagation*, Beijing, 1993, pp. 218-221.
 19. G. Ortgies, 'Frequency dependence of slant-path amplitude scintillations', *Proc. 20th Meeting of Olympus Propagation Experiment (OPEX)*, Darmstadt (D), 1993, pp. 156-164.
 20. U. Merlo, E. Fionda and J. Wang, 'Ground level refractivity and scintillation in space-earth links', *Appl. Optics*, **27**, 2246-2252 (1988).
 21. E. Vilar and J. Haddon, 'Measurement and modeling of scintillation intensity to estimate turbulence parameters in an Earth space path', *IEEE Trans. Ant. Propag.*, **32**, 340-346 (1984).
 22. F. S. Marzano and G. d'Auria, 'Estimation of intermittent scintillation on microwave links from meteorological data', *Alta Frequenza*, **6**, 94-97 (1994).
 23. D. Rouseff, 'Simulated microwave propagation through tropospheric turbulence', *IEEE Trans. Ant. Propag.*, **40**, 1076-1082 (1992).
 24. R. R. Rogers, C. A. Knights, J. D. Tuttle, W. L. Ecklund, D. A. Carter and S. A. Ethier, 'Radar reflectivity of the clear air at wavelengths of 5.5 and 33 cm', *Radio Sci.*, **27**, 645-659 (1992).
 25. A. Mood, F. Graybill and D. Boes, *Introduction to the Theory of Statistics*, New York, McGraw-Hill, New York, 1984.
 26. F. Rucker and F. Dintelmann, 'Effects of antenna size on OTS signal scintillations and their seasonal dependence', *Electron. Lett.*, **19**, 1032-1034, 1983.

Authors' biographies:

Geoffroy Peeters obtained his MS degree in electrical engineering in 1995 from the Université Catholique de Louvain, Louvain-la-Neuve, Belgium with a thesis on the statistical prediction of scintillation along earth-satellite microwave links. From February to June 1995 he was at the Department of Electronic Engineering of the University 'La Sapienza' in Rome within an Erasmus programme on electromagnetic propagation in turbulent atmosphere. Since

the end of 1995, he has been attending courses at I.R.C.A.M. in Paris, France, where he is presently pursuing doctoral research with a special focus on digital signal processing.

Frank Silvio Marzano received his laurea degree (cum laude) in electrical engineering (1989) and a PhD degree (1993) in applied electromagnetics from the University 'La Sapienza', Rome, Italy.

Since then, he has been the recipient of a fellowship of the Italian Space Agency and, presently, he has a Postdoctoral position with the Department of Electronic Engineering of 'La Sapienza' University, Rome, Italy. His current research concerns passive and active remote sensing of the atmosphere from airborne and spaceborne platforms, radiative transfer modelling of scattering media and scintillation analysis along satellite microwave links. Since 1990, he has been participating in many international projects on remote sensing and telecommunications (MAC-Europe in 1991, GPCP-AIP-2 in 1992, NASA PIP-2 in 1994 and GPCP-AIP-3 in 1995, COST-255 in 1996).

Dr Marzano received the Young Scientist Award of the XXIVth General Assembly of the International Union of Radio Science (URSI) in 1993.

Giovanni d'Auria was born in Rome, Italy, in 1931. He obtained his degree in electrical engineering from the University 'La Sapienza', Rome, Italy, in 1956 and a libera docenza degree in 1964, also from the same university.

He served in the Italian Air Force, working in ITAV Laboratories. He was then with Fondazione Ugo Bordoni as a researcher in the Antennas and Propagation Laboratory. He joined the Department of Electronics, University of Rome, in 1962 as an Assistant Professor, teaching applied electronics. In 1976 he was appointed Professor in the Chair of Antennas and Propagation and has been teaching this subject ever since. His current research concerns electromagnetic propagation in a turbulent atmosphere, microwave remote sensing of the atmosphere and the earth's surface, microwave radiometry of the atmosphere, and particularly of cloud systems.

Dr d'Auria is currently an official member of Comm. F of the Italian Committee of URSI.

Carlo Riva was born in Italy in 1965. He obtained his degree in electronic engineering in 1990 from the Politecnico di Milano with a graduating thesis related to optical fibres, after a stage with SIRTI SpA. From 1991 to 1994 he attended the doctorate course in electronic and communication engineering at the Politecnico di Milano in the propagation field with a special focus on scintillations.

In 1992 he attended a 3 month stage at the European Space Research and Technology Centre in Noordwijk (The Netherlands) working on scintillations. In 1993 he was with the Université Catholique de Louvain, in Louvain-la-Neuve (Belgium) for 2 months, carrying on research on the separation of turbulence and rain effects on satellite communication links.

Danielle Vanhoenacker-Janvier received her degree in electrical engineering in 1978 from the Université Catholique de Louvain (UCL) and her doctor in applied sciences in 1987 from the same University. Since 1978, she has worked at the Microwaves Laboratory UCL on atmospheric propagation at microwave and millimeterwave fre-

quencies. She has been involved in various COST projects of the EEC and in the OTS and Olympus propagation experiment of the European Space Agency. From 1986, she has been involved in the analysis and design of

microwave and millimeterwave active circuits. She is presently an Associate Professor at UCL, where she is teaching courses on electromagnetics, microwave active circuits design and telecommunication.